

SETTINGS OF THE GREAT SHRINE OF SAINT MAURICE – AG ALLOY – HIGH MEDIEVAL TIMES

Artefact name	Settings of the Great Shrine of saint Maurice
Authors	Romain. Jeanneret (Abbaye de St-Maurice, Saint-Maurice, Valais, Switzerland)
Url	/artefacts/1175/

≡ The object



Credit ABSM, J-Y. Glassey & M. Martinez.

Fig. 1: General and side views of the Great Shrine of saint Maurice, showing the location of the arcature settings of Fig. 2,



Credit ABSM, R. Jeanneret.

Fig. 2: Arcature settings located in Fig. 1,

≡ Description and visual observation

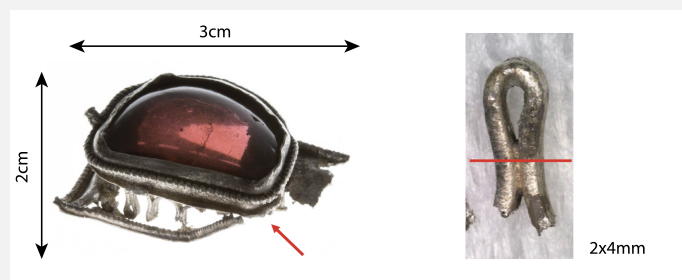
Description of the artefact	Set of arcature settings from the Great Shrine of saint Maurice. In large quantities (62 pieces) on the reliquary, these decorations have a structure showing a rationalization of the manufacturing process. Openwork plates, twisted wires and folded bands (arcatures) are welded together to form a decorative whole. The surfaces of these mounts seem to indicate a fire passage at the limit of the silver's fusion, which could be attributed to a copper salt soldering since the difference in fusion temperature between the solder and the alloy is very close.
Type of artefact	Religious goldsmithing
Origin	Northern continental Europe
Recovering date	Between 11th and 13th century
Chronology category	High medieval times

chronology tpq	<div><div>1000</div><div>A.D. ▾</div></div>
chronology taq	<div><div>1250</div><div>A.D. ▾</div></div>
Chronology comment	
Burial conditions / environment	Indoor atmosphere
Artefact location	Abbey of St Maurice, Saint-Maurice, Valais
Owner	Abbey of St Maurice, Saint-Maurice, Valais
Inv. number	Inv.2_Settings n°Bv35.02, Bv49.07 and Cv44.02
Recorded conservation data	

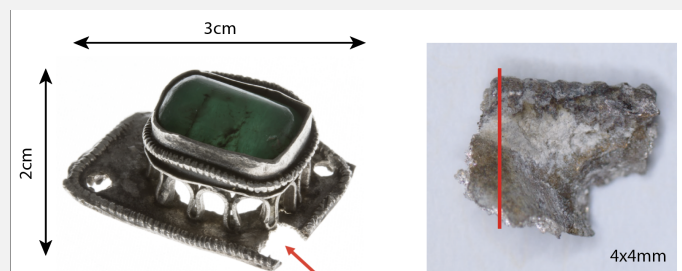
Complementary information

See Girardin (2015).

Study area(s)



Credit ABSM, R. Jeanneret.



Credit ABSM, R. Jeanneret.



Credit ABSM, R. Jeanneret.

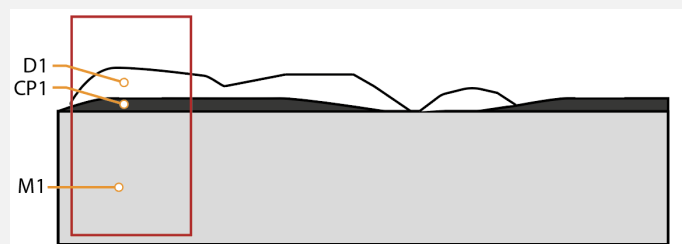
Fig. 3: Location of the analyzed fragments (3) of setting Bv35.02 and of the sampling area on the arcature tarnished fragment soldered on itself. Dimensions: 4 x 2 mm,

Fig. 4: Location of the analyzed tarnished fragment covered with deposits of cleaning products of setting Bv49.07 and of the sampling area. Assembly by solder between the bottom plate and the twisted wire. Dimensions: 4 x 4 mm,

Fig. 5: Location of the analyzed tarnished fragment of setting Cv44.02 and of the sampling area. Assembly by solder between the bottom plate and the twisted wire. Dimensions: 4 x 2 mm,

Binocular observation and representation of the corrosion structure

The schematic representation of Fig. 6 gives an overview of the corrosion structures encountered on the arcature settings from a first visual macroscopic observation.



Credit ABSM, R.Jeanneret.

Fig. 6: Stratigraphic representation of the corrosion structures of both settings Bv35.02, Bv49.07 and Cv44.02 by macroscopic and binocular observation with indication of the corrosion structure used to build the MiCorr stratigraphy of Fig. 7 (red rectangular),

≈ MiCorr stratigraphy(ies) – Bi

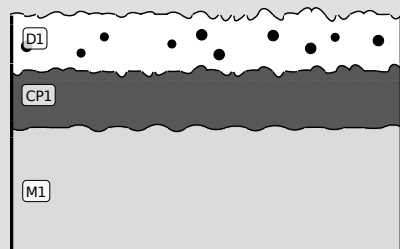


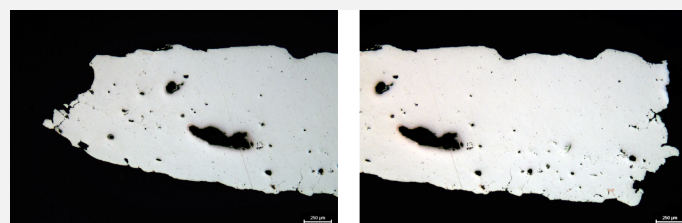
Fig.7: Stratigraphic representation of the corrosion structures of the Bv35.02, Bv49.07 & Cv44.02 settings observed macroscopically under binocular microscope using the MiCorr application with reference to Fig. 6. The characteristics of the strata are only accessible by clicking on the drawing that redirects you to the search tool by stratigraphy representation. Credit HE-Arc CR, N. Gutknecht.

≈ Sample(s)



Credit HEI Arc, S.Ramseyer.

Fig.8: SEM image (BSE mode, current 10nA) of the cross-section of the sample taken from setting Bv35.02 revealing partly the microstructure,



Credit HEI Arc, S.Ramseyer.

Fig.9: Micrograph of the cross-section of the sample taken from setting Bv49.07,

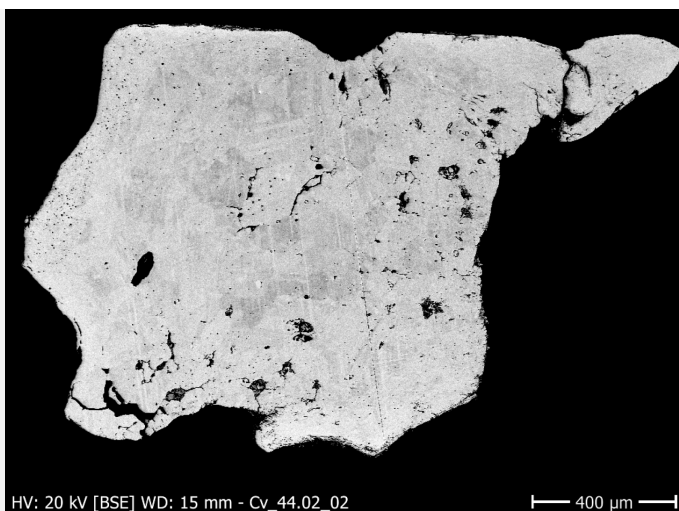


Fig. 10: SEM image (BSE mode, current 10nA) of the cross-section of the sample taken from setting Cv44.02 revealing partly the microstructure,

HV: 20 kV [BSE] WD: 15 mm - Cv_44.02_02

400 μm

Credit HEI Arc, S.Ramseyer.

Description of sample	Samples of fragments of arcature settings embedded (Figs. 8 to 10). These are transversal cut as shown on Fig. 3 to 5.
Alloy	Ag alloy
Technology	Hammered, wire twisted, annealed and welded
Lab number of sample	
Sample location	Abbey of St Maurice, Saint-Maurice, Valais
Responsible institution	Abbey of St Maurice, Saint-Maurice, Valais
Date and aim of sampling	18.09.2020

Complementary information

None.

✧ Analyses and results

Analyses performed:

Non-invasive approach

- XRF with handheld portable X-ray fluorescence spectrometer (NITON XL3t 950 Air GOLDD+, Thermo Fischer®). Precious mode, acquisition time 60s.

Invasive approach (on samples)

- Optical microscopy: the sample is polished, then it is observed on a numerical microscope LEICA DMLM in bright field.

- Metallography: the polished sample is etched in an oxygenated ammoniacal solution (10mL NH_3 25%+5mL H_2O_2 6%+10mL $(\text{NH}_4)_2\text{SO}_4$ 20%) and observed by optical microscopy in bright field.

- SEM-EDS: the sample is coated with a carbon layer and analyses are performed on a SEM-EDX JEOL equipped with a silicon-drift EDS Oxford detector with an accelerating voltage of 20 kV and probe current from a 1 to 10nA (to reveal the microstructure).

✧ Non invasive analysis

During a portable p-XRF analysis campaign, the base plate of setting number Av35.02 was studied. The result of this analysis seems to indicate a silver alloy of about 3wt% Cu. Traces of elements such as gold, lead, and iron were also found.

Metal

The metal of all settings is silver with a low percentage of copper (about 1wt% Cu). It validates XRF analyses. The difference in the percentage of copper compared to the XRF analyses (1wt% vs. 3wt% Cu) can be explained by a better accuracy of this other technique or more likely because it is a different element.

Welding zones are present, in particular for the Bv35.02 and Cv44.02 settings, only visible after etching (Figs. 11, 12 and 15). No clear difference in composition can be seen in these areas (Figs. 13 and 16). The grain structure (large polygonal grains, which may indicate recrystallization of the material(s)) is only visible in the SEM, BSE mode, and by increasing the beam intensity to 10nA (Figs. 8 and 10). Smaller grains are observed in the welding zones (Fig. 8).



Fig.11: Micrograph of Bv35.02 sample etched (to compare to Fig. 8),

Credit HE-Arc CR, C.Degrigny.



Fig. 12: Micrograph (detail) of the weld joint of the Bv35.02 cross-section after etching,

Credit HE-Arc CR, C.Degrigny.

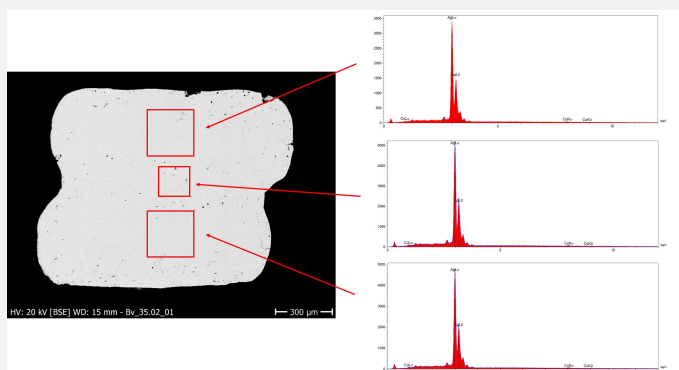
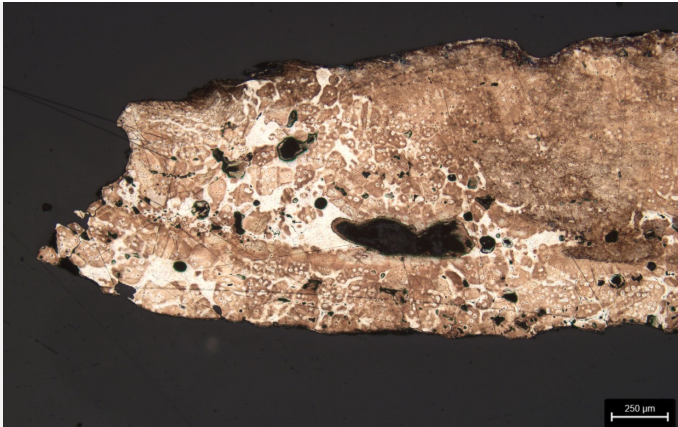


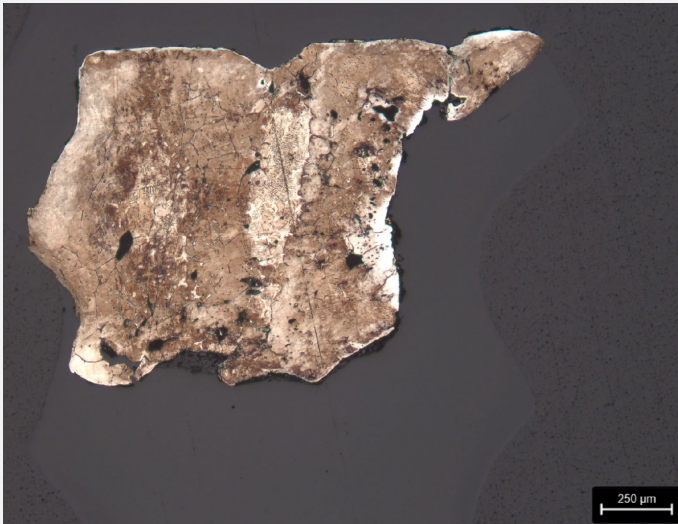
Fig.13: Location of EDS analyses on the cross-section of the Bv35.02 setting with associated spectra,

Credit HEI Arc, S.Ramseyer.

Fig.14: Micrograph of Bv49.07 sample etched. No EDS analysis was made,

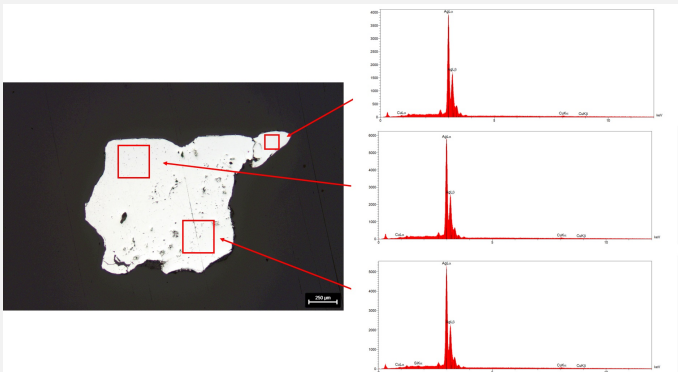


Credit HE-Arc CR, C.Degrigny.



Credit HE-Arc CR, C.Degrigny.

Fig.15: Micrograph of Cv44.02 sample etched (to compare to Fig. 10),



Credit HEI Arc, S.Ramseyer.

Fig.16: Location of EDS analyses on the cross-section of the Cv44.02 setting with associated spectra,

Microstructure	Recrystallized structure with large grains
First metal element	Ag
Other metal elements	Cu

Complementary information

None.

✖ Corrosion layers

The metal is covered with a thin layer of greyish and yellowish tarnish (CP1) on which residues of cleaning products are detected (D1). This tarnish has not been analyzed, but other work shows that the silver tarnish of the objects in the Treasury of the Abbey of Saint-Maurice usually consists of silver sulphide and silver chloride (Degrigny et al. 2015). This type of tarnishing is typical for silver alloys containing low copper content (Costa 2001, Graedel 1992 and Tissot et al. 2016). The metal of the settings is the site of intergranular corrosion (Wanhill, 2013) which appears to be limited to a thickness of 150-200 microns (Figs. 8 and 10).

Corrosion form	intergranular surface corrosion
Corrosion type	Silver tarnishing

Complementary information

None.

✧ MiCorr stratigraphy(ies) – CS

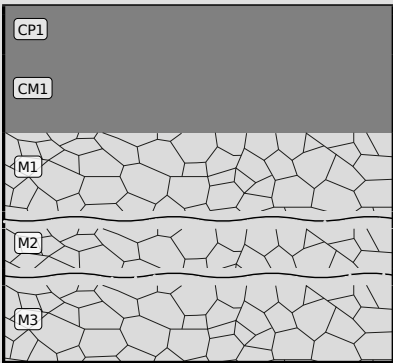


Fig.19: Stratigraphic representation of the sample taken from Bv35.02 in cross-section using the MiCorr application. The characteristics of the strata are only accessible by clicking on the drawing that redirects you to the search tool by stratigraphy representation. This representation can be compared to Fig. 8. Credit ABSM, R. Jeanneret.

✧ Synthesis of the binocular / cross-section examination of the corrosion structure

The observation in cross-section does not allow the identification of the surface deposits observed under the binocular microscope. This is probably due to the fact that they are localized and not very adherent. The surface tarnishing (CP1) is easily recognizable to the eye even though its thickness is very thin and not very visible in cross-section.

The CM1 layer, which corresponds to intergranular corrosion, is only visible in cross-section.

The weld zones are visible under the binocular microscope without being distinguishable from the core metal, but the etched cross-sections confirm their presence and distribution.

✧ Conclusion

The metal is a silver alloy with a low copper content (about 1 wt% Cu). Its corrosion layers are typical of silver with a very thin tarnish that has not been analyzed but is considered to be a mixture of silver sulfide and silver chloride. The metal surface suffers from a slight intergranular corrosion.

The metallographic study shows a microstructure that is difficult to interpret as indicated below.

The elemental analysis by EDS does not seem to show a more pronounced presence of copper in the soldered parts. This result goes against the hypothesis that the different parts of the settings would be assembled by soldering with copper salts or brazing by adding a silver pebble whose alloy would be close to the eutectic. Does this mean that the soldering is done without adding copper or silver flakes? This would indicate that the parts are pre-assembled by gluing and then fired at a temperature that places the alloy in a physical situation where welding takes place at the contact points without melting the rest.

This new hypothesis on the manufacture of the settings could explain the appearance of the surfaces of the pieces. Indeed, they seem very damaged, as if they had been heated close to fusion.

References

References on object and sample

1. Girardin, N. (2015). La châsse de saint Maurice. In: Mariaux, P.A dir., L'abbaye de Saint-Maurice d'Agaune 515-2015. Volume 2 - Le trésor. Ed. Infolio. Gollion, 73-85.

References on analytic methods and interpretation

2. Costa, V. (2001) The deterioration of silver alloys and some aspects of their conservation. In: Studies in Conservation 46 (Supplement-1), 18-34. <https://doi.org/10.1179/sic.2001.46.Supplement-1.18>.
3. Degriigny, C. et al. (2015) Local cleaning of tarnished Saint Candide reliquary head of the Treasury of Saint-Maurice Abbey, Valais (Switzerland) with the Pleco electrolytic pencil, e-preservation science, 12, 20-27.
4. Graedel, T. (1992). Corrosion mechanisms for silver exposed to the atmosphere, J. Electrochem. Soc. 139, 1963–1970.
5. Northover, S.M. & Northover, J.P. (2014) Microstructures of ancient and modern cast silver–copper alloys. Materials Characterization Volume 90, April 2014, Ed. Elsevier Amsterdam, 173-184.
6. Tissot, I. et al. (2016). Corrosion of silver alloys in sulphide environments: a multianalytical approach for surface characterisation. RSC Advances, 6, 51856-51863, doi:10.1039/C6RA05845K.
7. Wanhill, R. (2013) Stress corrosion cracking in ancient silver, Studies in Conservation, 58:1, 41-49, DOI: 10.1179/2047058412Y.0000000037.